Ab initio, variational transition state theory and quasiclassical trajectory study on the lowest $^2A'$ potential energy surface involved in the $N(^2D)+O_2(X^3\Sigma_g^-)\rightarrow O(^3P)+NO(X^2\Pi)$ atmospheric reaction

Miguel González,[a),b)] Irene Miquel, and R. Sayós[a),c)]
Departament de Química Física i Centre de Recerca en Química Teòrica, Universitat de Barcelona, C/ Marti i Franquès, 1, 08028 Barcelona, Spain

(Received 9 April 2001; accepted 21 May 2001)

A CASSCF and CASPT2 *ab initio* study has been carried out for the lowest $^2A'$ potential energy surface ($2\,^2A'$ PES) that correlates reactants and products of the $N(^2D)+O_2\rightarrow O(^3P)+NO$ reaction. All the stationary points have been characterized and along with a grid of more than 600 *ab initio* points have been fitted to an analytical function. Afterwards, this analytical PES has been employed to study the kinetics [variational transition state theory (VTST) and quasiclassical trajectory (QCT) methods] and dynamics (QCT method) of the reaction. Concerning the rate constants, a good agreement with the experimental values corresponding to the global deactivation of $N(^2D)$ has been obtained. This suggests that this reaction is responsible of most of the reactivity of the $N(^2D)+O_2$ system. NO vibrational distributions have also been calculated. Although there is not a good agreement between the theoretical and experimental values, preliminary results show that they can become quite close by taking into account the contribution of the $1\,^2A''$ PES. © *2001 American Institute of Physics.* [DOI: 10.1063/1.1385151]

I. INTRODUCTION

The reaction between the nitrogen atom in its first excited electronic state $N(^2D)$ and molecular oxygen in its ground-state $O_2(X\,^3\Sigma_g^-)$ has been the subject of a great interest in recent years because it is involved in the production of highly vibrationally excited NO present in the thermosphere. Moreover, metastable atomic nitrogen, $N(^2D)$, plays an important role in the chemistry of the nonequilibrium upper atmosphere and of systems employing nitrogen or air discharge plasmas.[1]

Reaction between $N(^2D)$ and O_2 can take place by means of two reactive channels

$$N(^2D)+O_2(X\,^3\Sigma_g^-)\rightarrow O(^1D)+NO(X\,^2\Pi) \quad \Delta H^0_{298\,K}=-41.4\,\text{kcal mol}^{-1}\ ,^{2,3} \tag{1}$$

$$\rightarrow O(^3P)+NO(X\,^2\Pi) \quad \Delta H^0_{298\,K}=-86.7\,\text{kcal mol}^{-1}.\ ^{2,3} \tag{2}$$

The overall rate constant of the reaction between $N(^2D)$ and O_2 (including both reactive channels and the $N(^2D)$ physical electronic quenching) has been measured by several authors[4–14] and at room temperature (298 K) a global rate constant of $5.2\times10^{-12}\,\text{cm}^3\,\text{molecule}^{-1}\,\text{s}^{-1}$ has been recommended.[15] Moreover, there are two experimental works[16,17] that provide information about the temperature dependence of the rate constant and the recommended[15] expression can be taken as: $k=9.7\times10^{-12}\exp(-185/T)$ $\text{cm}^3\,\text{molecule}^{-1}\,\text{s}^{-1}$ in the range of (210–465 K).

In a very recent paper[1] we have succeeded in reproducing these rate constant values by means of a complete active space second-order perturbation theory/variational transition state theory (CASPT2/VTST) study of reactions (1) and (2). We have considered the abstraction transition state of the $4\,^2A'$ potential energy surface [reaction (1)] and the corresponding one of the $2\,^2A'$, $3\,^2A'$, $1\,^2A''$, and $2\,^2A''$ potential energy surfaces [reaction (2)], without taking into account possible electronically nonadiabatic processes. From this study, we have concluded that the contribution of reaction (1) is negligible with respect to that of reaction (2), this last reaction probably being also dominant over the physical electronic quenching.

As regards the NO vibrational distributions, they have also been measured[18] showing an "inverted" distribution peaking at NO ($v'=7$) at $T=100$ K. In a recent theoretical paper[19] it has been obtained a qualitative agreement with these experimental results by means of quasiclassical trajectory (QCT) calculations on the two most important potential energy surfaces of reaction (2) ($2\,^2A'$ and $1\,^2A''$ PESs), excluding electronically nonadiabatic effects and considering a temperature of 500 K in the simulations.

The main purpose of this work is to present a detailed study of the lowest $^2A'$ surface ($2\,^2A'$ PES) involved in the $N(^2D)+O_2\rightarrow O(^3P)+NO(X\,^2\Pi)$ reaction. This PES is probably the most important one due to its very low energy barrier. We have carried out a CASSCF/CASPT2 *ab initio* study of this surface computing about 600 points that have been fitted by means of a many-body analytical expression. Afterwards, we have used this analytical PES to perform a VTST kinetic study and a QCT kinetic and dynamic study of reaction (2). Finally, a comparison with the experiments has been performed.

a)Authors to whom correspondence should be addressed.
b)Electronic mail: miguel@qf.ub.es
c)Electronic mail: r.sayos@qf.ub.es

II. METHODOLOGY

A. *Ab initio* methods

Potential energy surfaces of $^2A'(2)$, $^2A''(2)$, $^4A'$, and $^4A''$ symmetry (where between parenthesis is indicated the number of PESs of each symmetry) are involved in reaction (2). In a previous study of these surfaces[1] we have concluded that the most important ones for reactivity are the $2\,^2A'$ and the $1\,^2A''$ PESs. In this paper we will focus our attention in the full characterization of the $2\,^2A'$ PES.

This surface has been studied by means of the same *ab initio* methodology employed in the previous paper.[1] That is to say, we have carried out complete active space self-consistent field [CASSCF (17, 12)] calculations[20,21] and have computed the dynamic correlation energy by means of the CASPT2 method using the G2[22] correction to the Fock matrix and the standard correlation-consistent cc-pVTZ basis set of Dunning and co-workers[23] $(10s5p2d1f/4s3p2d1f)$. As our purpose was to study all the PESs involved in reaction (2), we have calculated the first three roots in C_s symmetry for the $^2A'$ states at CASSCF level using an equally weighted state averaged wave function, and CASPT2 G2 calculations were performed on the second and third roots. The first root of this symmetry and spin correlates the reactants in its ground state $[N(^4S)+O_2]$ with the products $[O(^3P)+NO]$ in the ground state, while the second and third roots correlate reactants and products of reaction (2). These two last electronic states are the ones in which we are interested to describe the structures, kinetics and dynamics of reaction (2). The calculations have been carried out using the MOLCAS 4.1[24] program. The characterization of some of the stationary points at CASSCF level has been carried out from the analytical gradients and numerical Hessian matrix as implemented in MOLCAS 4.1. However, when the use of these tools has not been successful at CASSCF level and in all cases at CASPT2 G2 level, the geometry optimization of the stationary points and the calculation of harmonic vibrational frequencies have been performed by fitting different sets of pointwise calculations using the SURVIBTM[25] program of molecular rovibrational analysis.

B. Analytical fit

A NOO′ many-body expansion[26] has been used to obtain an analytical representation of the $2\,^2A'$ PES, which can be written as

$$V(R_1,R_2,R_3)=V_N^{(1)}\cdot f(R_1,R_2,R_3)+V_{NO}^{(2)}(R_1)+V_{OO'}^{(2)}(R_2)+V_{NO'}^{(2)}(R_3)+V_{NOO'}^{(3)}(R_1,R_2,R_3), \quad (3)$$

where $V^{(1)}$, $V^{(2)}$, and $V^{(3)}$ are the one-, two-, and three-body terms, respectively. R_1 and R_3 are the N–O and N–O′ bond lengths and R_2 corresponds to the O–O′ bond length.

As the O and O′ atoms correlate with the ground electronic state in both reactants and products asymptotes, no one-body terms have been included for them. However, the *N* atom changes its electronic state from one asymptote to the other one [ground state, $N(^4S)$, in products and first excited electronic state, $N(^2D)$, in reactants]. As a consequence, a fully rigorous representation of the PES will be at least two-valued. Nevertheless, in order to get a relatively simple analytical form for the $2\,^2A'$ PES, we have used a single-valued representation[26,27] that reproduces properly the two atomic states in reactants and products asymptotes. This is achieved by including a one-body term, which consists on the product of the energy of the excited N atom relative to its ground state ($V_N^{(1)}$) and a switching function $[f(R_1,R_2,R_3)]$, whose value ranges between 0 (products) and 1 (reactants)

$$f(R_1,R_2,R_3)=\frac{1}{2}\left[1-\tanh\left(\frac{\alpha S'}{2}\right)\right], \quad (4)$$

where S' is expressed in terms of displacement coordinates $(\rho_j=R_j-R_j^0)$ with respect to a C_{2v}–ONO reference structure (i.e., $R_1^0=R_3^0$), and b_j' parameters that introduce the correct permutational symmetry of the PES with respect to the O–O′ exchange

$$S'=\sum_{j=1}^{3} b_j'\rho_j\,. \quad (5)$$

This one-body term ensures the correct asymptotic limits for reaction (2). The parameter α was optimized in the global fitting of the PES. This switching function does not ensure that a unique value of the energy is obtained for all the geometries of the system in which the three atoms are far away from each other. Nevertheless, this uniqueness is not crucial for the study to be performed on the $2\,^2A'$ PES because the three separated-atoms region will not be explored at all the energy conditions defined in the present study.

Extended-Rydberg potentials have been used to describe the two-body interaction for the NO and O_2 diatomic curves

$$V^{(2)}(R)=-D_e(1+a_1\rho+a_2\rho^2+\cdots)e^{-a_1\rho}. \quad (6)$$

Where $\rho=(R-R_e)$ is the diatomic internuclear displacement coordinate, D_e is the equilibrium dissociation energy, and R_e is the equilibrium bond length of the corresponding diatomic molecule. The a_i parameters have been determined by means of a nonlinear least-squares procedure, using the corresponding *ab initio* points and the experimental D_e and R_e values.

The three-body term consists of a *n*-order polynomial expressed in terms of symmetry-adapted coordinates [as in Eq. (5) for S' but now with other b_{ij} parameters] and a range function $T(S_1,S_2,S_3)$, which cancels the three-body term as one of the three atoms is separated from the other ones,

$$V_{NOO'}^{(3)}(R_1,R_2,R_3)=P(S_1,S_2,S_3)\cdot T(S_1,S_2,S_3), \quad (7)$$

where

$$P(S_1,S_2,S_3)=\sum_{i,j,k=0}^{1\leq i+j+k\leq n} c_{ijk}S_1^iS_2^jS_3^k, \quad (8)$$

being *i, j, k* positive integer numbers, and

$$T(S_1,S_2,S_3)=\prod_{i=1}^{3}\left[1-\tanh\left(\frac{\gamma_iS_i}{2}\right)\right], \quad (9)$$

with

$$S_i = \sum_{j=1}^{3} b_{ij}\rho_j . \tag{10}$$

The number of parameters in the three-body term is reduced owing to the use of the permutational symmetry (symmetry-adapted coordinates). From the set of linear $\{c_{ijk}\}$ and nonlinear $\{\gamma_i\}$ parameters, those which are associated to odd powers of S_3 (which is anti-symmetric with respect to the interchange of the O atoms) are identically zero. The nonzero parameters are determined by a weighted nonlinear least-squares procedure using the energies and geometries of a wide set of *ab initio* points.

The analytical expression of the $2\,^2A'$ PES has been obtained by means of the same set of programs[28,29] used in previous works of our group.[27,30,31]

C. Kinetics and dynamics methods

The rate constant values for reaction (2) resulting from the $2\,^2A'$ PES has been calculated in a wide range of temperatures using the variational transition state theory. The calculations have been performed considering the ICVT (improved canonical VTST) method and including the tunneling effect by means of the microcanonical optimized multidimensional (μOMT) correction (ICVT/μOMT method). Other corrections to the tunneling effect such as the SCT (small-curvature tunneling calculations) or the ZCT (zero-curvature tunneling calculations) have also been taken into account. However, there are no important differences in the value of the different rate constants obtained. These methods have been applied taking into account the $2\,^2A'$ analytical PES obtained from the set of *ab initio* points. The POLYRATE[32] program has been employed to perform all kinetic calculations.

The QCT method as implemented in the TRIQCT[33] program has been used to calculate the rate constant for reaction (2) at several temperatures and the vibrational distributions, $P(v')$, of NO arising from this reaction at 100 K. The accuracy of the numerical integration of Hamilton's differential equations has been verified by checking the conservation of total energy and total angular momentum along every trajectory, and performing back-integrations on sampling trajectories. The integration time step size chosen (i.e., 5×10^{-17} s) was found to achieve these conservation requirements for all the calculated trajectories. The trajectories were started and finished at a distance from the atom to the center-of-mass of the corresponding diatomic molecule of about 8.0 Å, ensuring that the interaction energy between fragments was negligible with respect to the available energy. For each temperature, both the relative translational energy, E_T, and vibrorotational levels of the O_2 molecule have been sampled according to a Maxwell–Boltzmann distribution. Final quantized internal distributions were obtained from vibrational radial action variables.

III. RESULTS

A. *Ab initio* study

The reaction between $N(^2D)$ and O_2 on the $2\,^2A'$ PES could occur through two different microscopic mechanisms: An abstraction mechanism and an insertion mechanism (see Fig. 1).

As regards abstraction mechanism, we have found the geometry, energy, and harmonic vibrational frequencies of the transition state implied in this process at the CASSCF and CASPT2 G2 levels. These calculations show the existence of a bent transition state (TS1) with a rather large bond distance between the N and O atoms while the distance between both O atoms is very similar to the O_2 equilibrium bond distance. Regarding the energy, this transition state presents a very small energy barrier at the CASPT2 G2 level (only 0.08 kcal mol^{-1}). Therefore, we can conclude that reaction between $N(^2D)$ and O_2 can take place through this mechanism practically without any energetic requirement. Moreover, and only when we include the dynamic correlation energy (CASPT2 G2 level), we have found two van der Waals (vdW) minima at both the entrance and exit valleys. The minimum in the entrance channel (MIN1) is only 0.47 kcal mol^{-1} more stable than reactants, while the one in the exit channel (MIN2) is located 2.82 kcal mol^{-1} below products.

The study of the insertion of the $N(^2D)$ atom into the O_2 bond is a much more complicated subject because of the existence of three conical intersections between the $1\,^2A'$ PES and the first excited $2\,^2A'$ PES along the insertion path.[34] These two states present three intersection seams in C_{2v} geometries, where they correspond to different symmetries ($^2A_1$ and $^2B_2$) and so they can cross. Two of these crossings are located near the transition state that makes possible the insertion mechanism. This fact has prevented us from finding an accurate geometry for this transition state by means of analytical gradients (because of the lack of energy convergence in some parts of the excited PES). Therefore, the geometry and energy of this transition state (TS2) at the CASSCF and CASPT2 levels has been found performing fittings of pointwise calculations using the SURVIBTM[25] program. We have not been able to compute its harmonic vibrational frequencies because of the impossibility of affording an accurate description of this transition state. Nevertheless, this stationary point is too energetic (22.5 kcal mol^{-1} at the CASPT2 level) to be involved in reactivity. Hence, in principle, the lower accuracy achieved in the description of this part of the PES does not represent a serious drawback for the purpose of the present work.

Another conical intersection between the $1\,^2A'$ and $2\,^2A'$ PESs is found at the end of the insertion path (ONO angles of about 120°). This conical intersection has already been reported in the bibliography[34–38] and it is located between two NO_2 minima [$NO_2(^2A_1)$ and $NO_2(^2B_2)$] that are present in the ground PES ($1\,^2A'$). Because of the peaked shape of this conical intersection (CI1), the energy of the $2\,^2A'$ PES increases in all directions from this intersection point and from an adiabatic point of view, it seems that this PES presents a minimum in this region. Therefore, in the

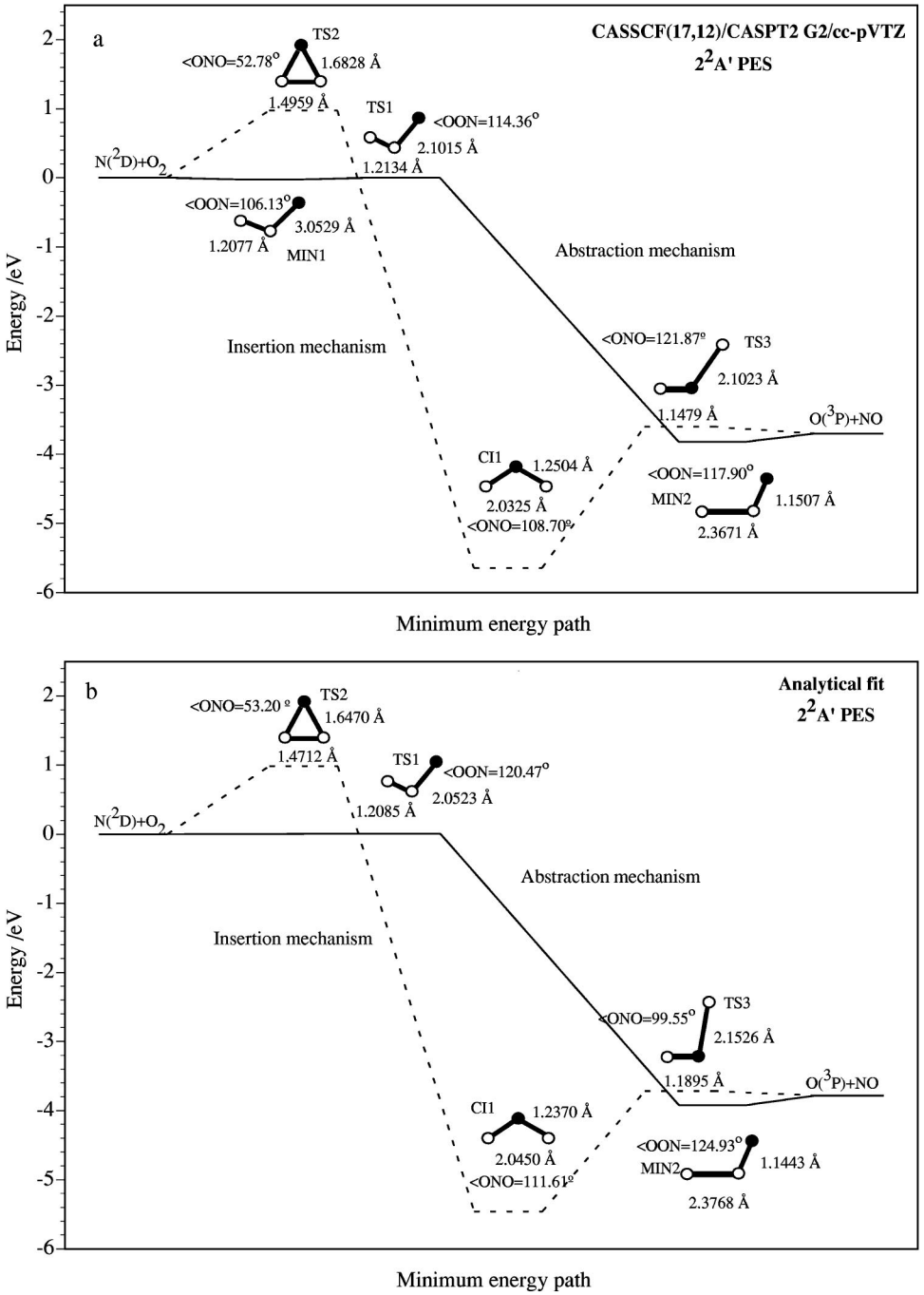

FIG. 1. Energy diagram of the stationary points located in the minimum energy path of the $2\ ^2A'$ PES: (a) *ab initio* level; (b) analytical PES. Energies are given in eV relative to reactants $[N(^2D)+O_2]$. In the analytical PES the conical intersection (CI1) really corresponds to a minimum (see text).

fitting procedure, we have considered this intersection point as a minimum. Finally, this intersection point correlates with products on the $2\ ^2A'$ PES by means of a bent transition state (TS3) that recovers the C_s symmetry and that is situated only 2.14 kcal mol^{-1} above products at the CASPT2 G2 level. The properties of all stationary points found at both CASSCF and CASPT2 G2 levels described in this section can be found in Table I.

The main conclusion of this *ab initio* study on the $2\ ^2A'$ PES is that while the abstraction mechanism can take place with a very small energetic requirement, the insertion mechanism is not easy at all because of the presence of a highly energetic transition state. The insertion mechanism would only be possible in case of nonadiabatic transitions taking place between the $2\ ^2A'$ and $1\ ^2A'$ PESs through the two conical intersections located not far from this transition state.

B. Analytical PES

The fitting of diatomic molecules (O_2 and NO) has been carried out using the corresponding *ab initio* points (20 and 25 points for O_2 and NO, respectively) and an extended Rydberg potential up to third-order for O_2 and up to fifth-order for NO has been employed. The values of equilibrium dissociation energy and bond distance used in the fitting procedure are the experimental ones because in this way we can reproduce exactly the exothermicity of reaction (2). The

TABLE I. Properties of the stationary points of the $2\,^2A'$ PES.

	R_{NO}/Å	R_{OO}/Å	<NOO/°	ω_i/cm^{-1}	E/kcal mol^{-1} [a]
Reactants $[N(^2D)+O_2]$					
CASSCF		1.2177		1541.74	0
CASPT2 G2		1.2091		1586.18	0
Analytical fit		1.2075		1610.1	0
Products $[O(^3P)+NO]$					
CASSCF	1.1587			1895.63	−102.33
CASPT2 G2	1.1543			1904.45	−85.02
Analytical fit	1.1508			1887.6	−87.28
Minimum in the entrance channel (MIN1) (C_s)[b]					
CASPT2 G2	3.0529	1.2077	106.13	1629 (ω_{O-O}), 21(ω_b), 41(ω_{N-O})	−0.47 (−0.32)
Saddle point of the abstraction mechanism (TS1) (C_s)					
CASSCF	1.9110	1.2310	104.74	339.34i(ω_a), 288.78(ω_b), 1385.28(ω_s)	6.65 (6.84)
CASPT2 G2	2.1015	1.2134	114.36	179i(ω_a), 339(ω_b), 1511(ω_s)	0.08 (0.45)
Analytical fit	2.052	1.208	120.5	200i(ω_a), 198(ω_b), 1488(ω_s)	0.19 (0.30)
Minimum in the exit channel (MIN2) (C_s)[b,c]					
CASPT2 G2	1.1507	2.3671	117.90	1881(ω_{N-O}), 192(ω_b), 570(ω_{O-O})	−2.82 (−1.76)
Analytical fit	1.144	2.377	124.9	1913(ω_{N-O}), 218(ω_b), 318(ω_{O-O})	−3.11 (−2.31)
	$R_{NO'}$/Å	$R_{NO''}$/Å	<ONO/°	ω_i/cm^{-1}	E/kcal mol^{-1} [a]
Saddle point of the insertion mechanism (TS2) (C_{2v})					
CASSCF	1.7066	1.7066	53.14		37.30
CASPT2 G2	1.6828	1.6828	52.78		22.50
Analytical fit	1.647	1.647	53.2	713i(ω_a), 879i(ω_b), 814(ω_s)[d]	22.75
Conical intersection in the insertion path (CI1) (C_{2v})					
CASSCF	1.2626	1.2626	109.12		−118.64
CASPT2 G2	1.2504	1.2504	108.7		−130.20
Analytical fit	1.237	1.237	111.6		−125.83
Saddle point that connects products with the conical intersection (TS3)[c] (C_s)					
CASSCF	1.1528	1.8784	114.97	724.18i($\omega_{N-O''}$), 372.77(ω_b), 1829.36($\omega_{N-O'}$)	14.20 (14.60)
CASPT2 G2	1.1479	2.1023	121.87	350i($\omega_{N-O''}$), 160($\omega_{bO'NO''}$), 2048($\omega_{N-O'}$)	2.14 (2.58)
Analytical fit	1.1895	2.1526	99.5	258i($\omega_{N-O''}$), 244($\omega_{bO'NO''}$), 1761($\omega_{N-O'}$)	1.53 (1.67)

[a]Energy referred to reactants. Between parentheses is given E+ZPE, where ZPE is the zero-point energy.
[b]The van der Waals minima are only present at the CASPT2 G2 level. The minimum in the entrance channel is not found in the analytical PES.
[c]In the case of the minimum of the exit channel, the value of energy is referred to products, the same as in the case of the saddle point that connects products with the conical intersection.
[d]This stationary point has two imaginary frequencies. It has not been possible to find the harmonic frequencies at *ab initio* level (see text).

root-mean-square deviations (RMSD) for the diatomic curves of O_2 and NO are 0.39 and 0.53 kcal mol^{-1}, respectively. The optimal extended Rydberg parameters of each diatomic molecule are given in Table II and the spectroscopic constants derived from them are given in Table III.

Regarding the three-body term, we have used as reference structure an average of the geometries of TS1, TS2, and CI1, and the value of the one-body term is taken as $V_N^{(1)} = 2.3835$ eV (corresponding to the experimental energetic requirement for the excitation process $N(^4S) \rightarrow N(^2D)^3$). The *ab initio* data employed to determine the three-body parameters are the following: (a) Energy and geometry of the *ab initio* stationary points; (b) 491 *ab initio* points in the part of abstraction mechanism (C_s symmetry, NOO region) and 144 *ab initio* points in the part of insertion mechanism (C_{2v} symmetry, ONO arrangement); (c) about 1000 points interpolated between the *ab initio* points by means of a bicubic-splines procedure that allow us to eliminate spurious structures in the entrance and exit valleys. Moreover, all points have been properly scaled shifting the value of their energy to reproduce the exothermicity of reaction (2). Although most of *ab initio* points are concentrated near the stationary points, the asymptotes have also been widely explored to provide a good description of the PES around the minimum energy path (MEP). The whole set of points was fitted to a sixth-order polynomial. In Table II are shown the optimal parameters of the present $2\,^2A'$ analytical PES three-body term. There are 87 polynomial coefficients, but as 35 coefficients are equal to zero, due to the permutational symmetry of the system, this leads to 52 coefficients to be optimized, 50 of which are linear and 2 nonlinear (γ_1 and γ_2).

In general, there is a good agreement between the *ab initio* properties of the stationary points and those resulting from the fitting. For the 391 *ab initio* points that being in the abstraction part of the PES (NOO region) are located until 0.8 eV above reactants, the global RMSD is of 1.86

TABLE II. Optimal parameters of the $2\ ^2A'$ analytical PES.

One-body parameters

$V_N^{(1)}$/eV	α/Å^{-1}	b_1'	b_2'	b_3'
2.3835	1.543 60	−1	3	−1

Two-body parameters

Species	D_e/eV	R_e/Å	a_1/Å^{-1}	a_2/Å^{-2}	a_3/Å^{-3}	a_4/Å^{-4}	a_5/Å^{-5}
O–O	5.2132	1.2075	5.458 19	7.581 88	5.115 49		
N–O	6.6144	1.1507	3.848 32	0.007 46	0.909 85	−6.264 02	4.291 64

Three-body parameters[a]

c_{000}	0.759 335	c_{102}	−1.669 42	c_{022}	0.424 288	c_{104}	0.919 137	c_{240}	0.424 977
c_{100}	1.280 81	c_{030}	−0.659 994	c_{004}	−0.154 127	c_{050}	0.373 377	c_{222}	1.808 65
c_{010}	0.418 072	c_{012}	−0.375 803	c_{500}	2.721 23	c_{032}	1.657 81	c_{204}	0.890 525
c_{200}	5.933 91	c_{400}	6.756 66	c_{410}	14.4835	c_{014}	−1.619 73	c_{150}	−0.265 530
c_{110}	3.170 44	c_{310}	26.3444	c_{320}	17.3547	c_{600}	0.409 072	c_{132}	2.150 69
c_{020}	−0.276 262	c_{220}	6.700 19	c_{302}	−2.845 79	c_{510}	2.744 96	c_{114}	−0.092 706 4
c_{002}	0.188 926	c_{202}	−4.224 69	c_{230}	−12.3871	c_{420}	9.024 16	c_{060}	0.020 804 6
c_{300}	8.049 03	c_{130}	−4.341 13	c_{212}	−7.979 77	c_{402}	−1.135 59	c_{042}	−0.751 648
c_{210}	16.4968	c_{112}	−2.663 71	c_{140}	−0.202 443	c_{330}	−8.681 17	c_{024}	0.489 769
c_{120}	0.130 245	c_{040}	−0.278 559	c_{122}	−1.922 45	c_{312}	−6.158 21	c_{006}	0.288 162

$R_1^0=R_3^0$/Å	R_2^0/Å	γ_1/Å^{-1}	γ_2/Å^{-1}	γ_3/Å^{-1}
2.4685	1.7786	3.968 31	2.488 64	0.0

b_{ij} $i,j=1,2,3$

$$\begin{pmatrix} \sqrt{(1/2)} & 0.0 & \sqrt{(1/2)} \\ 0.0 & 1.0 & 0.0 \\ \sqrt{(1/2)} & 0.0 & -\sqrt{(1/2)} \end{pmatrix}$$

[a]Units for the coefficients are eV Å$^{-(i+j+k)}$.

kcal mol^{-1} and for the 422 points situated until 1.3 eV above reactants the global RMSD is 2.25 kcal mol^{-1}. As regards, the insertion part of the PES (ONO region), the RMSD is not so good (7.3 kcal mol^{-1} for 144 *ab initio* points). However, the reactivity will not result from this part of the PES under the conditions explored due to the high-energy barrier of the insertion mechanism. The geometry and energy of the most important stationary points of the analytical PES are very coincident with the properties of the *ab initio* ones (Table I and Fig. 1). The contour diagrams at several NOO angles (110°, 140°, and 180°) and the contour diagram for the ONO arrangement using the Jacobi coordinates where R is the diatomic (O–O) internuclear distance and r is the distance from the nitrogen atom (N) to the center-of-mass of the diatomic molecule are shown in Fig. 2.

C. Rate constants

The thermal rate constant through the $2\ ^2A'$ PES of reaction (2) has been calculated within the 100–1000 K range of temperatures at ICVT level of theory. To take into account that there are two equivalent oxygen atoms in the saddle point, the ICVT rate constant associated to the PES has been multiplied by two (statistical factor). Furthermore, the μOMT tunneling correction has been considered. The ICVT results have been compared with the rate constants calculated by means of a QCT study at 100, 200, 300, 400, 500, and 1000 K. The values obtained by the statistical methods and by the QCT method are very similar. Regarding the tunneling effect, it is only important at the lowest temperature explored (100 K) where we can appreciate an increase of a 25% in

TABLE III. Spectroscopic constants of the diatomic molecules.

Species	D_e/eV[a]	R_e/Å[a]	ω_e/cm^{-1}	$\omega_e x_e$/cm^{-1}	B_e/cm^{-1}	α_e/cm^{-1}
O_2						
Analytical fit	5.2132	1.2075	1610.1	12.554	1.445 30	0.0152
Experimental[b]	5.2132	1.2075	1580.2	11.981	1.445 63	0.0159
NO						
Analytical fit	6.6144	1.1508	1887.6	13.569	1.704 47	0.0193
Experimental[b]	6.6144	1.1508	1904.2	14.100	1.671 95	0.0171

[a]The value of D_e and R_e included in the fit are the experimental ones. For this reason both values (the analytical fit and the experimental ones) are the same. The *ab initio* CASSCF(17,12)/CASPT2 G2/cc-pVTZ values for D_e and R_e are: 5.3362 eV and 1.2091 Å for O_2, and 6.4912 eV and 1.1543 Å for NO, respectively.
[b]Reference 39.

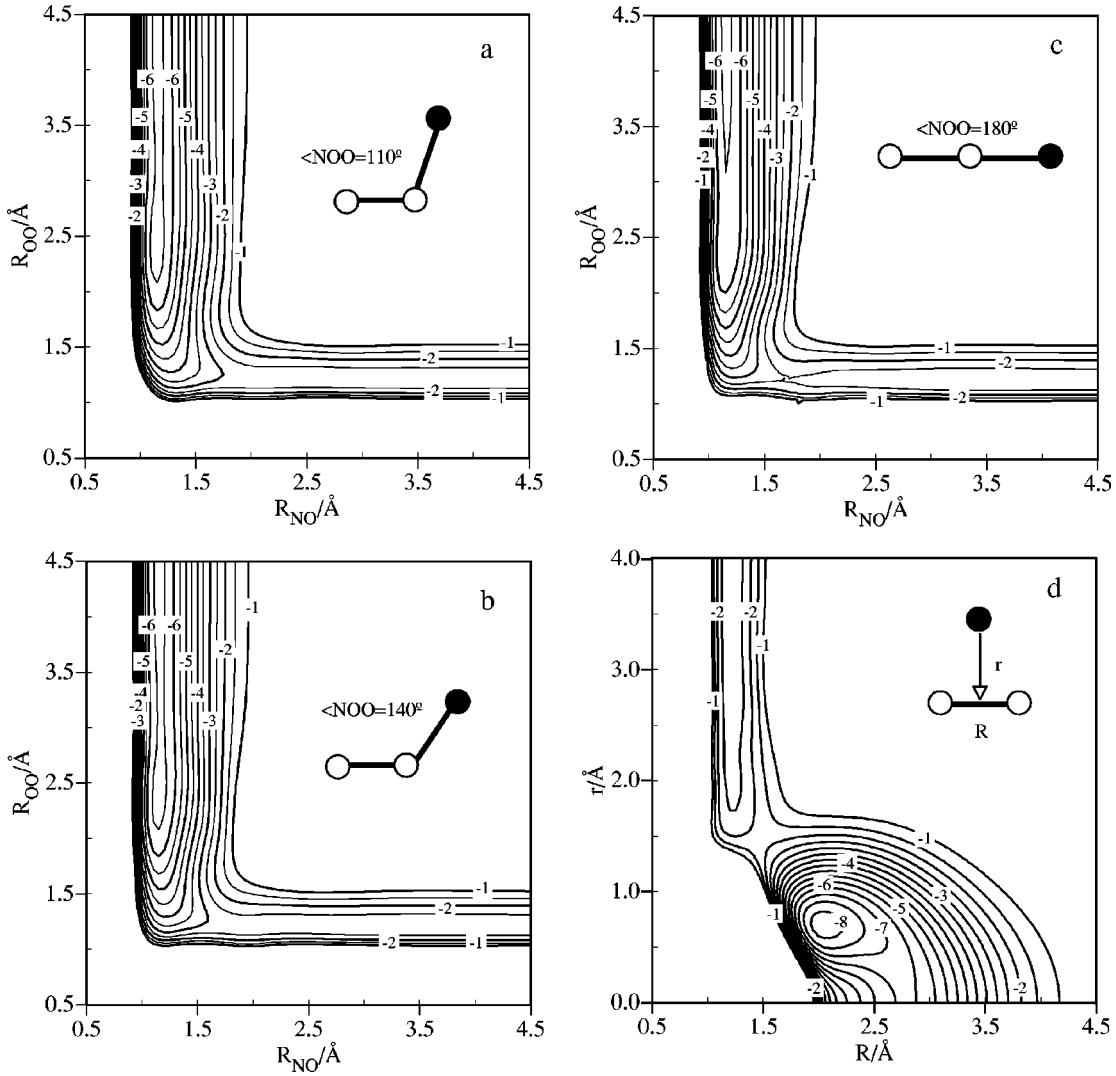

FIG. 2. Contour diagrams of the $2\,^2A'$ analytical PES at different ∠NOO angles: (a) 110°, (b) 140°, (c) 180°, and (d) NO_2 (C_{2v} arrangement described using Jacobi coordinates). The contours are depicted in increments of 0.5 eV and the zero of energy is taken in $N(^4S)+O(^3P)+O(^3P)$.

reactivity due to this effect. The importance of tunneling, however, decreases rapidly as temperature increases because heavy atoms and low-imaginary frequency of TS1 are involved in reaction (2). Table IV and Fig. 3 show the values of the rate constant for the $2\,^2A'$ PES at different levels of theory.

From the electronic states adiabatic correlation between reactants and products and neglecting electronically nonadiabatic effects, it comes out that the global rate constant for reaction (2) can be expressed as

$$k(2)=k(2\,^2A')+k(1\,^2A''), \tag{11}$$

where the ratio between the electronic partition functions of the corresponding saddle point and that of the reactants has been taken as

$$\frac{Z_{el,TS}}{Z_{el,N(^2D)}\cdot Z_{el,O_2}}=\frac{2}{[6+4\exp(-12.536/T)]\cdot 3}. \tag{12}$$

In this case and to avoid conceptual problems, the rate constant for reaction (2), $k(2)$, has been expressed in a different way to the previous paper.[1] The value of 12.536 K that appears in Eq. (12) corresponds to the energy of the excited spin–orbit (SO) state of the $N(^2D)$ atom ($^2D_{3/2}$) relative to the ground SO state ($^2D_{5/2}$), 8.713 cm^{-1}, divided by the Boltzman constant.

For reaction (2) there are six PESs ($2\,^2A'$, $3\,^2A'$, $1\,^2A''$, $2\,^2A''$, $3\,^4A'$, and $3\,^4A''$) that adiabatically correlate reactants and products. However, we have shown in a very recent

TABLE IV. Rate constants of the $2\,^2A'$ analytical PES at different levels of theory.[a]

T/K	ICVT	ICVT/μOMT	QCT[b]
100	5.85×10^{-13}	7.86×10^{-13}	$(6.37\pm0.15)\times10^{-13}$
200	1.50×10^{-12}	1.61×10^{-12}	$(1.50\pm0.07)\times10^{-12}$
300	2.35×10^{-12}	2.43×10^{-12}	$(2.35\pm0.05)\times10^{-12}$
400	3.16×10^{-12}	3.22×10^{-12}	$(3.14\pm0.11)\times10^{-12}$
500	3.97×10^{-12}	4.02×10^{-12}	$(3.66\pm0.11)\times10^{-12}$
1000	7.92×10^{-12}	7.94×10^{-12}	$(8.57\pm0.15)\times10^{-12}$

[a]Units are $cm^3\,molecule^{-1}\,s^{-1}$.
[b]Statistical errors correspond to one standard deviation.

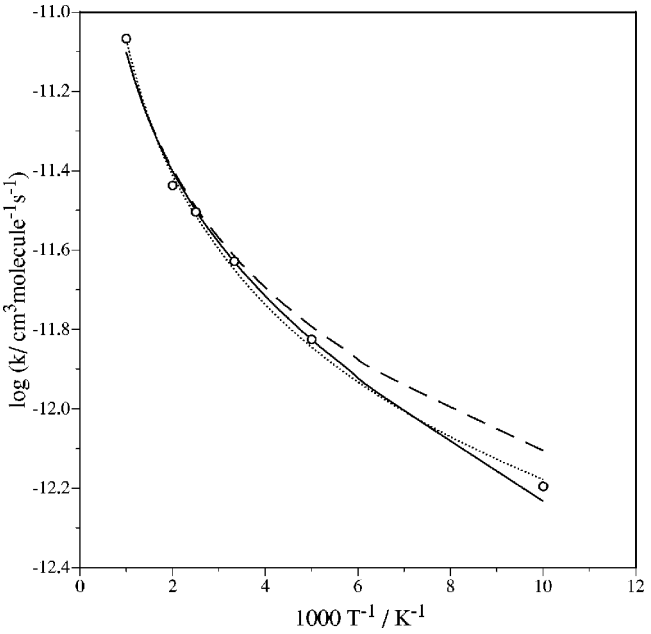

FIG. 3. Arrhenius plot of the calculated rate constants for the $2\ ^2A'$ analytical PES: (——) ICVT, (— — —) ICVT/μOMT, (···○···) QCT. The QCT error bars correspond approximately to the size of the symbol.

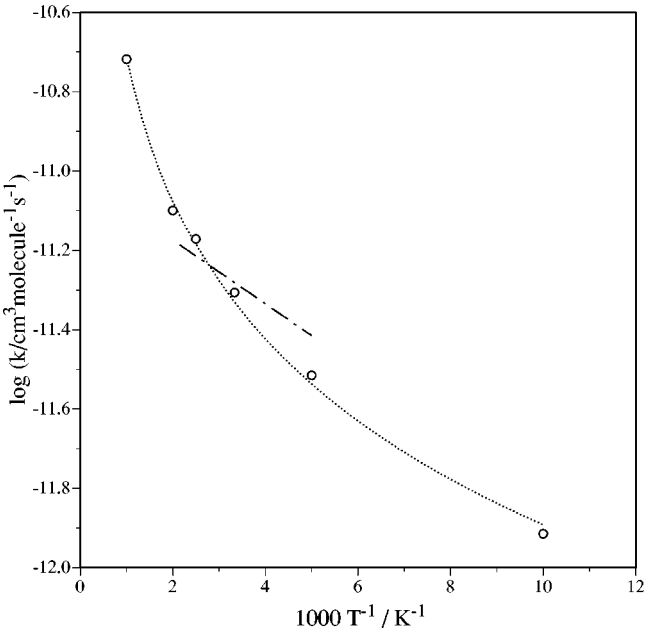

FIG. 4. Arrhenius plot of the rate constants of reaction (2). (···○···) QCT values (the QCT error bars correspond approximately to the size of the symbol), (— - — -) recommended experimental data (Ref. 15). In the case of the experimental results the two reactive channels and the physical electronic quenching are included. That is to say, they correspond to the global rate constant for the deactivation of $N(^2D)$ (see text).

paper[1] that four of these PESs ($3\ ^2A'$, $2\ ^2A''$, $3\ ^4A'$, and $3\ ^4A''$) have high enough energy barriers to not be involved in reactivity at temperatures below 1000 K. At these temperatures, the only important contributions to reactivity are the ones from the $2\ ^2A'$ and the $1\ ^2A''$ PESs. Taking this fact into account, we have calculated the rate constant of reaction (2) at QCT level, considering that only the $2\ ^2A'$ and $1\ ^2A''$ PESs are involved in the reactivity. The value of $k(T)$ at the QCT level for the $1\ ^2A''$ PES has been estimated from the value of $k(T)$ at the QCT level for the $2\ ^2A'$ PES and the relationship at the ICVT level between $k(T)$ for the $2\ ^2A'$ PES and $k(T)$ for $1\ ^2A''$ PES[1]. Table V and Fig. 4 show both the values of the rate constant for reaction (2) at the QCT level and the experimental global ones. We can see that QCT rate constants are in good agreement with the experimental ones in the range of temperatures in which they have been calculated (210–465 K). The experimental values also include the process of deactivation of $N(^2D)$ by means of the physical electronic quenching. Because of the good agreement between the experimental values and the theoretical ones [that only include the deactivation of $N(^2D)$ by means of reaction (2)], we can conclude that this reaction dominates over the electronic quenching.

TABLE V. Rate constants of reaction (2).[a]

T/K	$k(T)$ reaction (2) ICVT[b]	$k(T)$ reaction (2) QCT	$k(T)$ global[c] Experimental[d]
100	6.96×10^{-13}	1.22×10^{-12}	
200	2.40×10^{-12}	3.06×10^{-12}	3.85×10^{-12}
300	4.17×10^{-12}	4.94×10^{-12}	5.24×10^{-12}
400	5.93×10^{-12}	6.74×10^{-12}	6.11×10^{-12}
500	7.69×10^{-12}	7.96×10^{-12}	
1000	1.65×10^{-11}	1.91×10^{-11}	

[a]Units are $cm^3\ molecule^{-1}\ s^{-1}$.
[b]$k(T)$ has been calculated taking into account the $2\ ^2A'$ and the $1\ ^2A''$ PES of our previous paper (Ref. 1). See text.
[c]Including both reactive channels [reactions (1) and (2)] and the electronic physical quenching of $N(^2D)$.
[d]Reference 15.

D. Dynamical properties

As refers to the reaction mode, we have shown (Sec. II A) the existence of two possible reaction pathways through which the system can evolve along the $2\ ^2A'$ PES. However, all the reactive trajectories calculated from an initial translational energy of 0.05 eV until 1.0 eV are direct and evolve

TABLE VI. NO vibrational distributions from the reaction (2) at 100 K.[a]

v'	QCT	Experiment[b]
0	0.00	0.0136
1	0.00	0.0249
2	0.00	0.0437
3	0.00	0.0722
4	0.0005 ± 0.0005	0.1120
5	0.0056 ± 0.0017	0.1580
6	0.0619 ± 0.0057	0.1870
7	0.1945 ± 0.0101	0.1530
8	0.2027 ± 0.0103	0.1240
9	0.2410 ± 0.0112	0.0551
10	0.2390 ± 0.0112	0.0284
11	0.0548 ± 0.0053	0.0144
12	0.00	0.0072
13	0.00	0.0035
14	0.00	0.0016

[a]Populations are normalized to unity.
[b]Reference 18.

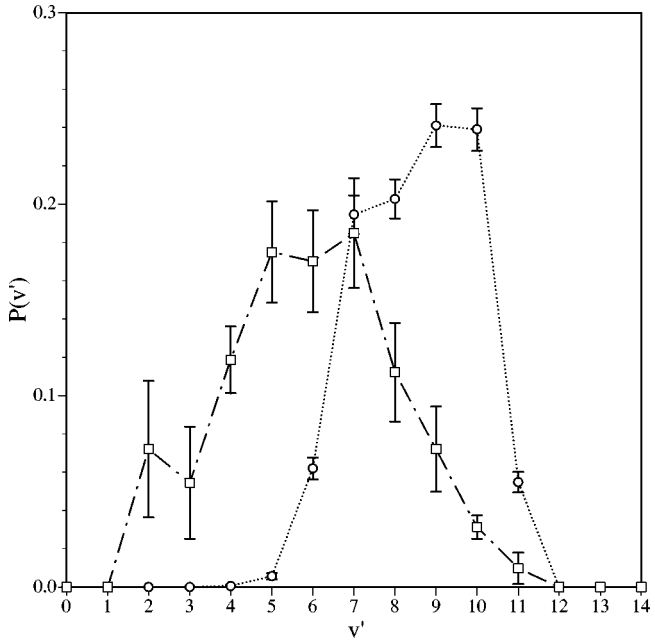

FIG. 5. NO vibrational distributions for reaction (2) at 100 K. (···○···) QCT values obtained from the $2\,^2A'$ analytical PES, (—- □—-) experimental values (Ref. 18).

through the abstraction mechanism. This fact is not strange since the saddle point implied in the insertion mechanism is too energetic (22.5 kcal mol^{-1}) to be involved in reactivity.

The NO vibrational distribution arising from the $2\,^2A'$ analytical PES at 100 K has also been calculated and is indicated in Table VI and Fig. 5. This distribution is clearly inverted and peaked at $v'=9$ (being $\langle v' \rangle$ equal to 8.55) as expected for a reaction with a high exothermicity. All the thermodynamically accessible vibrational levels are populated. This vibrational distribution has also been compared with the experimental one.[18] In this case, the agreement with the experimental results is not good, since the experimental vibrational distribution of products is peaked near $v'=7$. In a recent theoretical paper[19] the vibrational distributions have also been calculated using the QCT method, taking into account the $2\,^2A'$ and $1\,^2A''$ PESs, but at a temperature of 500 K. In this case the agreement with the experimental results at 100 K is better. This fact implies that the $1\,^2A''$ PES has also an important role in reaction (2), as expected.

In fact, we have shown[1] that the $1\,^2A''$ PES has also low enough energy barriers (either in the abstraction or in the insertion mechanism) to be important in reactivity. Moreover, in case the insertion mechanism takes place and the system evolves in a significant way through a minimum, the vibrational distributions would be colder and so more similar to the experimental ones. In spite of the existence of conical intersections along the reaction pathway, it is not probable that at 100 K the system evolves in a significant extent through electronically nonadiabatic transitions. Hence, the inclusion of the $1\,^2A''$ PES in the theoretical treatment will probably lead to a less excited NO vibrational distribution and a better comparison with experiment.[40] On the other hand, the possible existence of some relaxation in the measured vibrational distribution can not be completely ruled out.

IV. SUMMARY AND CONCLUSIONS

In this work we have carried out a detailed study of the lowest PES ($2\,^2A'$ surface) implied in the reaction of N(^2D) with O_2 to produce NO and O(^3P). Along with the $1\,^2A''$ PES the studied PES is the most involved in the reactivity due to its very low-energy transition state. We have characterized all its stationary points at the CASSCF(17, 12) and CASPT2 G2 levels using the cc-pVTZ basis set and have shown that the possibility of an insertion mechanism on the $2\,^2A'$ PES is essentially closed due to its highly energetic transition state. This mechanism would only be possible in case of electronically nonadiabatic transitions involving the $1\,^2A'$ and the $2\,^2A'$ PESs in the C_{2v} region. In this region, these two PESs have different symmetry and they present three crossings, two of them near the insertion transition state and another one between the ground and the first excited state of the NO_2 molecule.

We have also calculated a grid of ~600 *ab initio* points of the $2\,^2A'$ PES and they have been fitted to an analytical expression. The goodness of the fit has been validated by the small RMSD and by the quite accurate reproduction of all the *ab initio* stationary points properties.

The rate constants resulting from the $2\,^2A'$ PES have been calculated at the VTST level and by means of the QCT method, showing a good agreement in the whole range of temperatures (100–1000 K) where they have been calculated. The tunneling effect has also been included by means of the μOMT correction and it has been shown that this effect is not important at temperatures above 200 K. An estimation of the rate constant of reaction (2) has been carried out at the QCT level and a good agreement with the global (reactions plus physical electronic quenching) measured results has been obtained. From this agreement we can conclude that reaction (2) dominates over the electronic quenching. This is in accord with what was found in a very recent CASPT2/VTST study of our group, the contribution of reaction (1) to the reactivity being negligible due to its large energy barrier.

Finally, a QCT study of reaction (2) has been carried out at different initial translational energies (0.05–1.0 eV), showing that only the (direct) abstraction mechanism takes place. Moreover, we have obtained the vibrational distribution of NO arising from the $2\,^2A'$ PES at 100 K. The lack of agreement between this result and the experiment probably comes out from the fact that the $1\,^2A''$ PES should also be included in the calculation as it also has a very small energy barrier. Because of this, the same type of detailed study that we have carried out here for the $2\,^2A'$ PES is now in progress for the $1\,^2A''$ PES.

ACKNOWLEDGMENTS

This work has been supported by the ''Direction General de Enseñanza Superior (Programa Sectorial de Promoción General del Conocimiento)'' of the Spanish Ministry of Education and Culture (DGES Project PB98-1209-C02-01). Fi-

nancial support from the European Union (INTAS Project 99-00701) and the ''Generalitat de Catalunya'' (Autonomous Government of Catalonia) (Project 2000SGR 00016) is also acknowledged. One of the authors (I.M.) also thanks the ''Generalitat de Catalunya'' for a ''Beca de Formació d'Investigadors'' (Predoctoral Research Grant). The authors are also grateful to the ''Center de Computació i Comunicacions de Catalunya (C^4 (CESCA/CEPBA))'' for providing a part of the computer time.

[1] M. González, I. Miquel, and R. Sayós, Chem. Phys. Lett. **335**, 339 (2001), and references therein.
[2] M. W. Chase, Jr., C. A. Davies, J. R. Downey, Jr., D. J. Frurip, R. A. McDonald, and A. N. Syverud, J. Phys. Chem. Ref. Data Suppl. **1**, 14 (1985).
[3] S. Bashkin and J. O. Stonner, Jr., in *Atomic Energy Levels and Grotrian Diagrams 1* (North-Holland, Amsterdam, 1975), Vol. 1.
[4] F. Kaufman, ''Atmospheric reactions involving neutral constituents—an evaluation,'' paper presented at the American Geophysical Union Meeting, San Francisco, December, 1968.
[5] G. Black, T. G. Slanger, G. A. St. John, and R. A. Young, J. Chem. Phys. **51**, 116 (1969).
[6] C. L. Lin and F. Kaufman, J. Chem. Phys. **55**, 3760 (1971).
[7] T. G. Slanger, B. J. Wood, and G. Black, J. Geophys. Res. **76**, 8430 (1971).
[8] D. Husain, L. J. Kirsch, and J. R. Wiesenfeld, Faraday Discuss. Chem. Soc. **53**, 201 (1972).
[9] D. Husain, S. K. Mitra, and A. N. Young, J. Chem. Soc., Faraday Trans. 2 **10**, 1721 (1974).
[10] J. E. Davenport, T. G. Slanger, and G. Black, J. Geophys. Res. **81**, 12 (1976).
[11] M. P. Iannuzzi and F. Kaufman, J. Chem. Phys. **73**, 4701 (1980).
[12] B. Fell, I. V. Rivas, and D. L. McFadden, J. Phys. Chem. **85**, 224 (1981).
[13] L. G. Piper, M. E. Donahue, and W. T. Rawlins, J. Phys. Chem. **91**, 3883 (1987).
[14] P. D. Whitefield and F. E. Hovis, Chem. Phys. Lett. **135**, 454 (1987).
[15] J. Herron, J. Phys. Chem. Ref. Data **28**, 1453 (1999).
[16] Y. Shihira, T. Suzuki, S. Unayuma, H. Umemoto, and S. Tsunashima, J. Chem. Soc., Faraday Trans. **90**, 549 (1994).
[17] L. E. Jusinski, G. Black, and T. G. Slanger, J. Phys. Chem. **92**, 5977 (1988).
[18] W. T. Rawlins, M. E. Fraser, and S. M. Miller, J. Phys. Chem. **93**, 1097 (1989).
[19] M. Braunstein and J. W. Duff, J. Chem. Phys. **113**, 7406 (2000).
[20] B. O. Roos, P. R. Taylor, and P. E. M. Siegbahn, Chem. Phys. **48**, 157 (1980).
[21] B. O. Roos, in *Advances in Chemical Physics: Ab Initio Methods in Quantum Chemistry-II*, edited by K. P. Lawley (Wiley, Chichester, 1987), Vol. LXIX, p. 399.
[22] K. Andersson, Theor. Chim. Acta **91**, 31 (1995).
[23] T. H. Dunning, Jr., J. Chem. Phys. **90**, 1007 (1989).
[24] K. Anderson, M. R. A. Blomberg, M. P. Fülscher *et al.*, MOLCAS Version 4.1, Lund University, Sweden (1998).
[25] W. C. Ermler, H. C. Hsieh, and L. B. Harding, Comput. Phys. Commun. **51**, 257 (1988).
[26] J. N. Murrell, S. Carter, S. C. Farantos, P. Huxley, and A. J. C. Varandas, in *Molecular Potential Energy Surfaces* (Wiley, New York, 1984).
[27] M. González, R. Valero, and R. Sayós, J. Chem. Phys. **113**, 10983 (2000).
[28] M. González and R. Sayós, DIATOMFIT (unpublished program).
[29] R. Sayós and M. González, SM3FIT (unpublished program).
[30] M. González, J. Hernando, J. Millán, and R. Sayós, J. Chem. Phys. **110**, 7326 (1999).
[31] R. Sayós, C. Oliva, and M. González, J. Chem. Phys. **113**, 6736 (2000).
[32] R. Steckler, Y.-Y. Chuang, E. L. Coitiño *et al.*, POLYRATE—Version 7.0, University of Minnesota, Minneapolis, 1996.
[33] R. Sayós and M. González, TRIQCT (unpublished program).
[34] R. Sayós, C. Oliva, and M. González (in preparation).
[35] A. J. Merer and K.-E. J. Hallin, Can. J. Phys. **56**, 838 (1978).
[36] G. Hirsch and R. J. Buenker, Can. J. Chem. **63**, 1542 (1985).
[37] C. P. Blahous, B. F. Yates, Y. Xie, and H. F. Schaefer III, J. Chem. Phys. **93**, 8105 (1990).
[38] E. Leonardi, C. Petrongolo, G. Hirsch, and R. J. Buenker, J. Chem. Phys. **105**, 9051 (1996).
[39] K. P. Huber and G. Herzberg, in *Molecular Spectra and Molecular Structure* (Van Nostrand Reinhold, New York, 1979), Vol. 4.
[40] M. González, I. Miquel, and R. Sayós (in preparation).